WELDING RESEARCH

SUPPLEMENT TO THE *WELDING JOURNAL*, AUGUST 1993
Sponsored by the American Welding Society and the Welding Research Council

Investigation into the Fatigue Strength of Fillet Welded Assemblies of E-36-4 Steel As a Function of the Penetration of the Weld Subjected to Tensile and Bending Loads

Tests revealed a critical degree of incomplete fusion below which this discontinuity had no significant effect on the fatigue life of the weldment

BY J. J. JANOSCH

ABSTRACT. This study is aimed at evaluating the effect of incomplete penetration on the fatigue behavior of fillet welded assemblies subjected to tension and bending. Its purpose is to evaluate more precisely the conditions of slow extension of microcracks during the initiation stage. The preferred sites for crack initiation at the weld root or the weld toe were determined by using the finite element method. The experimental program, including 120 fatigue tests, was conducted on 10 mm and 30 mm thick E-36-4 steel plates welded with gas metal arc welding (GMAW) and shielded metal arc welding (SMAW) processes. The results evidenced a propagation phase of short cracks, which may represent 30 to 90% of the fatigue life, and the existence of a critical size of incomplete joint penetration below which the incomplete penetration had no significant effect on the fatigue life of fillet welded assemblies subjected to tension and bending.

The numerical calculations, made with the finite element method, have permitted the modeling of the crack propagation paths as a function of the size of incomplete penetration and the determination of the relations KI = f(a/t) for each zone of failure of the fillet weld.

The formulation of the analytical model for estimating the fatigue life of fillet welded assemblies enabled us to take into account the geometrical aspect, the evolution of the shape of crack front from the initiation stage through to the failure, and the fraction of crack opening defined by Elber (to introduce the amplitude of the effective stress intensity factor, ΔKeff, inherent in this type of welded joint).

The analysis of the results showed the effectiveness of the analytical modeling, which allowed the slow propagation phase of microcracks to be taken into account, and gave a satisfactory estimate of the fatigue life whatever the zone of failure and the welding process used.

KEY WORDS

Fatigue Strength
Fillet Welds
E-36-4 Steel
Root Penetration
Tensile Load
Bending Load
Microcrack Extension
Finite Element Model
Fracture Mechanics
Failure Simulation

J. J. JANOSCH is with the Institut de Soudure, Ennery, France.

Introduction

Welded constructions (ships, pressure vessels, vehicles, etc.) have made great strides during the last decades. This was favored by a constant improvement in the quality of the materials used and by a better understanding of the mechanical behavior of welded constructions. By now, often as a result of an over conservative design approach, full penetration at the root is specified for fillet welded assemblies, with ultrasonic testing. This approach considerably increases the fabrication time and cost of welded structures. With a view to evaluating the desirability of this approach, we have studied the influence of an incomplete root-penetration on the fatigue behavior of assemblies containing load-carrying welds.

Earlier research work carried out at the Institut de Soudure (the French Institute of Welding) on fillet welded assemblies of E-36-4 steel (to AFNOR Standard), joined by GMAW process and subjected to uniaxial tensile loads (Ref. 1) had shown the existence of the following:

1) A critical size of incomplete root penetration below which the lack of penetration no longer affects the fatigue behavior (2a/t = 0.5; 2a = incomplete penetration; t = thickness of welded plates).

2) A stage of slow extension of microcracks propagating from a notch tip (at the toe of weld bead), which may represent 30 to 80% of the fatigue life, depending on the applied stress amplitude.

The present study is aimed at evaluating more precisely the conditions of slow propagation of microcracks that develop from the toe of the weld, and at modeling the fatigue behavior of fillet welded assemblies as a function of the size of incomplete root penetration in the case of combined tension and bending loads (Ref. 2).

Preliminary Numerical Analysis

This preliminary phase of numerical calculations is aimed at defining for the fillet welded assemblies the preferred crack-initiation sites at the toe and the root of welds subjected to tension and bending loads — Fig. 1. Two-dimensional calculations were conducted by applying the linear theory of elasticity with special consideration given to the plane strain conditions.

The results were analyzed in terms of the evolution of the local stresses σ1 (main stresses I are expressed in the main coordinate for the stresses) in each sensitive zone of the weld. The calculations were conducted as a function of the geometrical parameters that define the fillet welded assembly: incomplete penetration (2a), toe angle (θ), throat thickness (H/t), thickness ratio of the welded plates (T/t)); and the conditions of loading applied to the weld (variation of the ratio of nominal tensile stress to the nominal bending stress, σNT/σNfl).

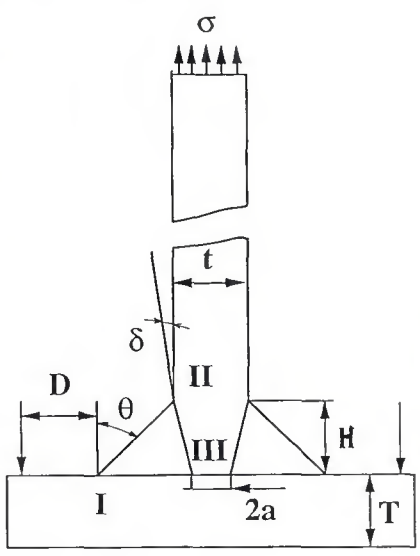

Fig. 1 — Schematic of fillet welded assembly showing fracture Zones I, II and III and geometrical parameters used in calculations. Refer to Table 1 for dimensions of assemblies.

Calculations by the finite element method determined three basic geometries of fillet welded assemblies in which it was possible to obtain a crack initiation in one of the sensitive zones of the welded joint. These "optimized" geometries are shown in Table 1.

Experimental Results

Experimental Conditions

The experimental program was conducted on a 10- and 30-mm thick E-36-4 grade steel (to AFNOR standard). The fillet welded assemblies were produced by using two popular welding processes: semiautomatic gas metal arc welding (GMAW), and shielded metal arc welding (SMAW) with basic electrodes.

The chemical analyses and mechanical properties of the base and filler metals are shown in Table 2. The fatigue tests were performed with computer-controlled hydraulic machines at constant force amplitudes and a ratio of R = Pmin/Pmax = 0.1. Nine weld geometries were adopted for each welding process — Figs. 2, 3.

With a view to "penalizing" the root of the weld, all the assemblies were produced in the flat position. As a matter of fact, such a procedure leads to an improvement of the local geometry of the weld toes.

Detection of the Fatigue Microcracks

The detection and monitoring of the fatigue microcracks extending from the weld toes (Zones I, II) were done by using micro-strain gauges (type KIOWA KFC1 D19, with an area of 1 mm2) positioned along the weld toes. For each fatigue test, this method permits the determination of the depth of microcrack (a) ($0.05 < a < 1$ mm), the evolution of the crack at the surface of the weld toe (2c), and the nominal crack opening load (P opening).

These experimental data have permitted the definition of the fracture zone (Zones I, II) of the geometric characteristics of the weld and of the loading conditions as a function of the welding process as follows:

1) The evolution of the shape of the crack front a/c = f(a/t) — Fig. 4.

2) The relative fraction of crack opening (Fig. 5) as defined by Elber (Ref. 3).

$$U = \frac{\sigma_{max} - \sigma_{op}}{\sigma_{max} - \sigma_{min}} \text{ Fig. (5)} \qquad (1)$$

3) The conditions of slow propagation of microcracks for depths of "a" between 0.05 mm and 1 mm — Figs. 6, 7.

Synthesis of the Experimental Study

Evolution of the Fatigue Microcracks Extending from the Weld Toes

The use of micro-strain gauges attached onto the weld toe permitted the detection of small cracks from the initiation stage (a0 = 0.05 mm) through to a depth of 1 mm into the weld.

The comparative analysis of the measurements made on the fillet welded assemblies produced by pulsed GMAW or by SMAW with basic electrodes produced in each case a distinct evolution of the shape of the crack front.

Table 1 — Three Basic Geometries of the Test Assemblies

σN tension = 1 (MPa)	Geometrical Parameters						σ1 (MPa)		
Welded Assemblies	t (mm)	T/t	θ	D (mm)	H/t	2a (mm)	Zone I	Zone II	Zone III
1	10	1	45°	75	0.5	10	27	4.7	1
2	10	3	60°	16.5	0.5	10	1.12	4.05	2.18
3	10	3	30°	22	0.5	10	2.65	2.78	3.16

Table 2 — Properties and Chemistries of the Base and Filler Metals

Material	C (%)	Mn (%)	Si (%)	P (%)	A1 (%)	S (%)	Re (MPa)	Rm (MPa)	A (%)	Kcv (J/cm²)
Base metal E364	0.16	1.47	0.43	0.013	0.05	0.002	405	562	33	184 (−20°C)
Filler metal φ 1 mm 1st pass (+Atal gas)	0.06	0.9	0.45	0.025		0.025	460	550	27	90 (−20°C)
Filler metal φ 1.6 mm (Atal gas) 2nd pass	0.06	1.6	0.5	0.02		0.02	590	650	24	50 (−20°C)
Filler metal Basic electrodes 0 = 4 mm	0.07	0.9	0.5	0.01		0.010	500	580	27	110 (−30°C)

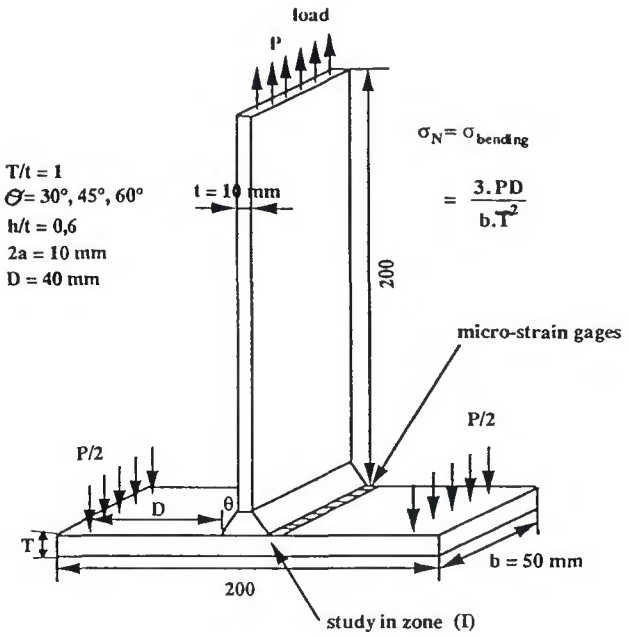

Fig. 2 — Schematic of welded assembly showing the placement of the strain gauges for the study of Zone 1.

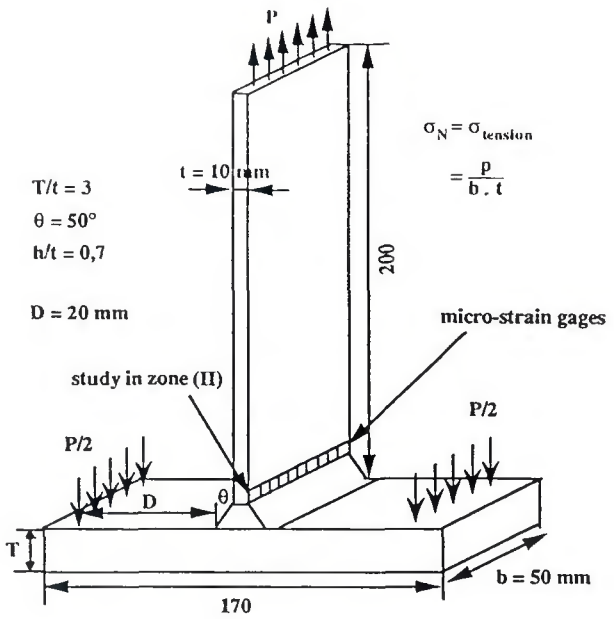

Fig. 3 — Schematic of weld assembly showing the placement of strain gauges for study of Zone II.

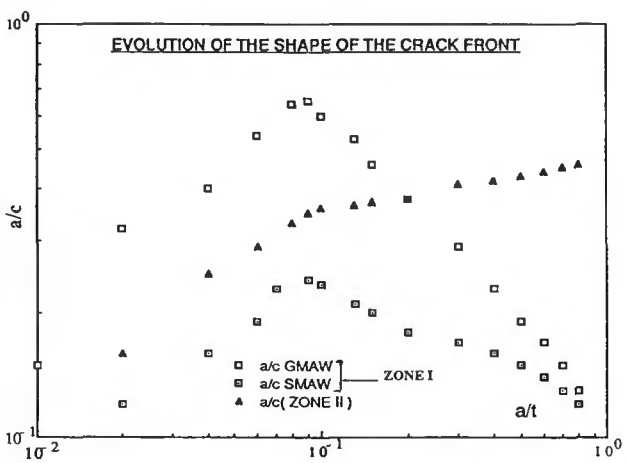

Fig. 4 — Diagram showing the evolution of the shape of the crack front.

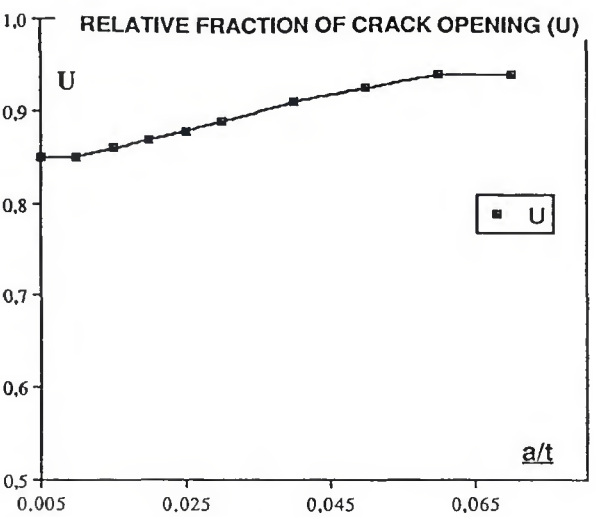

Fig. 5 — Diagram of relative fraction of crack opening.

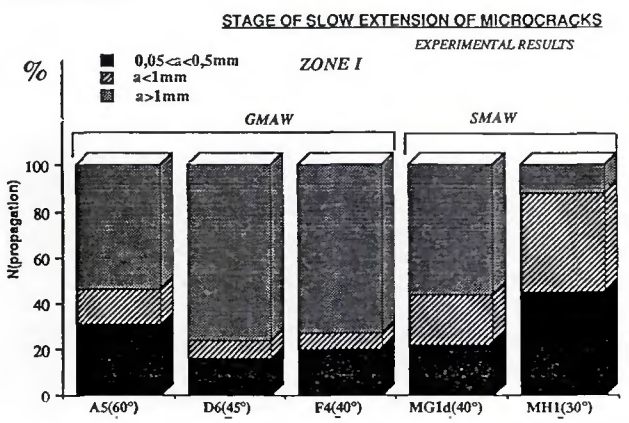

Fig. 6 — Extension of microcracks in Zone I.

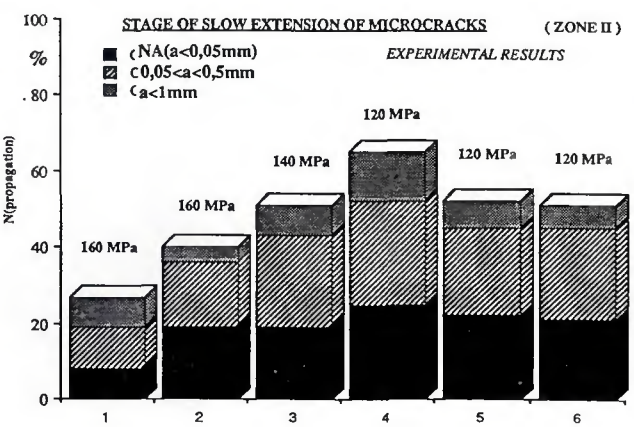

Fig. 7 — Extension of microcracks in Zone II.

This could be associated with the local geometry of the weld toe, which was more severe when the joints were welded manually, or with the proportion of microdiscontinuities (undercuts, microflaws) along the weld toes, which was more important when the joints were welded with the basic electrode.

The data obtained from the testing of the weld showed a microcrack propagation phase (from 0.05 to 1 mm depth into the weld), which may represent 30 to 90% of the fatigue life of the fillet welded assemblies — Figs. 6, 7. This propagation phase was more important in the case of test pieces welded with covered electrodes.

The evolution of the form of the crack front depended on the local state of the stress near the crack tip. In the case of the SMAW welding process, the small toe radii induced sharper notches, which increased the cyclic strain gradient and then affected the elliptical form of the crack during the fatigue tests. In this case, the crack was more elliptical and the proportion of fatigue life for obtaining a 1 mm depth in the weld was therefore more important when SMAW was used.

The data obtained from the testing in Zone I showed a relationship linking the toe angle (θ) with the conditions of evolution of the micro cracks. The proportion of fatigue life for reaching 1-mm depth in the weld increased for the SMAW assemblies when the macroscopic geometrical perturbation became more marked (that is, when θ increased). In the case of the GMAW assemblies, the opposite phenomenon was observed.

The proportion of fatigue life for reaching 1-mm depth in the weld increased when the amplitude of the applied stress decreased. Near the endurance limit (defined at 2 million cycles), this propagation phase averaged 50 to 60% of the fatigue life in the propagation of the fillet welded assemblies.

Effect of Incomplete Root Penetration

The data obtained from the testing in Zone I of the weld showed that there was no incidence of incomplete root-penetration when the thickness of the welded plates was equal to t = T = 10 mm. In that case, the fracture of the welded joint occurred at the weld toe in spite of the presence of incomplete fusion equal to the thickness of the welded plates (2a = 10 mm) — Fig. 8.

The fatigue study carried out in Zone II of the weld evidenced an interaction between the crack path (from Zone II) and the size of the incomplete fusion at the root as detailed below.

1) With an incomplete penetration size smaller than 2a/t = 0.3–0.4, the crack propagated from the toe of the weld into the thickness of the plate subjected to tension — Fig. 9.

2) When the incomplete penetration was 0.4 < 2a/t < 0.8, a deviation of the crack towards the incomplete fusion was observed. This deviation occurred when the crack reached a depth of a/t = 0.3–0.4. Then, the fatigue failure extended from the root — Fig. 10. The test results showed in this case a simultaneous propagation of fatigue cracks at the toe and the root of the weld.

3) For a critical size of incomplete penetration 2a/t greater than 0.8, a crack arrest was observed in Zone II when the crack reached a depth between 1.5 and 4 mm, depending on the applied load level. The fatigue failure occurred then at the root of the weld.

4) Although the fracture modes of the welded joints were distinct, the observed difference in fatigue life was hardly significant. This was probably associated with the residual deflection of the welded plates (induced by the welding sequence), which increased the scatter of test results.

The study of the fatigue behavior of the weld root (Zone III) also showed a relationship between the weld fracture mode and the size of the incomplete penetration. The following was observed:

1) At 2a/t < 0.7, crack propagation was displaced towards Zone I of the weld — Fig. 11A.

2) At 0.7 < 2a/t < 0.9, there was simultaneous propagation at the root and in Zone I of the weld toe, Fig. — 11B.

3) At 2a/t > 0.9, the assembly yielded at the root of the weld.

A marked decrease in the fatigue life was observed on this type of assembly (θ = 30 deg; T/t = 3; t =10 mm) when the fatigue failure of the welded joint extended solely from the root. In that case, the incomplete fusion at the root was evaluated at 2a/t = 0.8–0.9 (t = 10 mm).

Thus, the synthesis of the test results showed the existence of a critical size of incomplete penetration below which the incomplete penetration will not exert any significant effect on the fatigue life of the fillet welded assemblies subjected to tension and bending. For the assemblies produced with the GMAW and SMAW processes, the critical value was estimated at 2a/t = 0.8 (t = 10 mm; T/t = 3; q = 30–60 deg).

All the research work conducted on the fillet welded load carrying joints showed that the most restrictive stress condition for admitting a critical size for the incomplete root penetration corresponded to a uniaxial tension loading (Ref. 1).

In this case, the critical size of incomplete penetration below which the incomplete penetration no longer af-

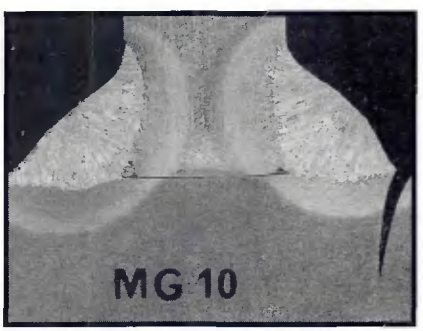

Fig. 8 — Weld crack at the toe regardless of incomplete root penetration.

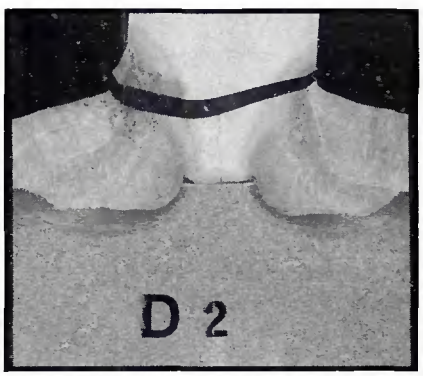

Fig. 9 — Crack propagates from the toe through the thickness of the member.

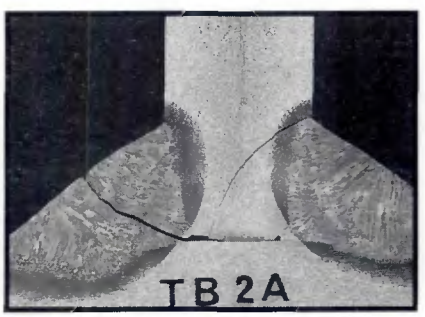

A

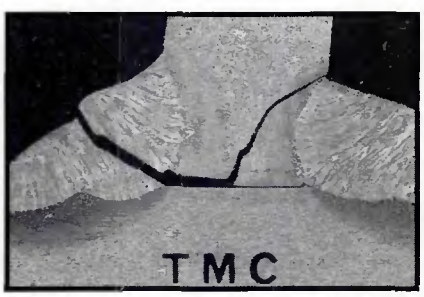

B

Fig. 10 — Simultaneous propagation of cracks from the toe and the root of the weld. A — GMAW process; B — SMAW process.

fected the fatigue behavior was 2a/t = 0.5 (t = thickness of welded plates).

Modeling of Fatigue Life

The numerical calculations were conducted at the Institut de Soudure by using the procedure of the SYSTUS finite element analysis method developed by FRAMASOFT + CSI.

The two-dimensional calculations were made by applying the linear theory of elasticity with special consideration of the plane-strain conditions and a homogeneous material free from welding residual stresses. The stress intensity factors (KI, KII) were determined by using a singular element at the crack tip — Fig. 12.

Crack Path Modeling

The experimental study conducted on fillet welded assemblies subjected to tension and bending has revealed the existence of several fatigue failure modes. These failure modes were affected by the weld geometry, the loading conditions, and the size of incomplete penetration.

To achieve the modeling of the fatigue life of the welded assemblies, it is necessary to predict the crack path as a function of the aforementioned parameters.

For defining the crack deviation angle (α) after each propagation increment (Zones I, II or III of the weld), we have chosen the energy criterion defined by Sih (Ref. 4). By knowing the values of the stress intensity factors KI and KII at the crack tip, the strain energy density S could be computed.

For an isotropic, homogeneous material, this energy density is expressed by

$$S = a_{11}k_I^2 + 2a_{12}\ k_I k_{II} + a_{22}k_{II}^2 \qquad (2)$$

(in a two dimentional stress condition).

In the case of plane strain

$$a_{11} = \frac{1}{16\mu}(3 - 4\nu - \cos\alpha)(1 + \cos\alpha)$$

$$a_{12} = \frac{1}{8\mu}\sin\alpha(\cos\alpha - 1 + 2\nu) \qquad (3)$$

$$a_{22} = \frac{1}{4\mu}(1-\nu)(1-\cos\alpha) + (3\times\cos\alpha - 1)(1-\cos\alpha)\frac{E}{2(1+\nu)}$$

where ν = Poisson's ratio, E = Young's modulus, μ = shear modulus $E/2(1+\nu)$, α = angle between the predicted direction and the true direction of the crack (already defined).

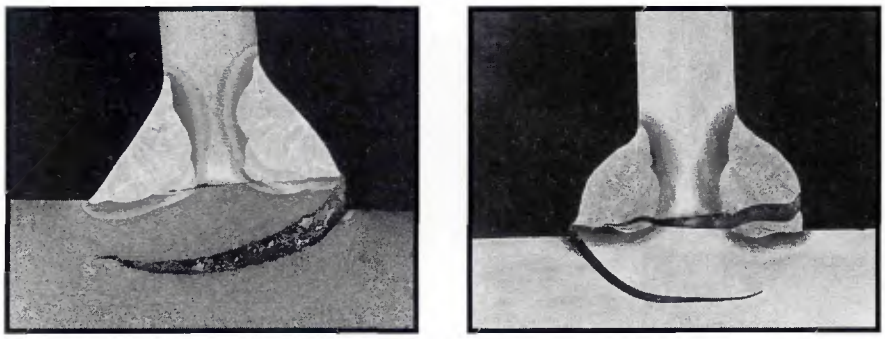

Fig. 11 — Relationship between weld fracture mode and the size of incomplete root penetration. A— Crack propagates towards Zone I; B — Crack propagates simultaneously from the tow and the root of the weld.

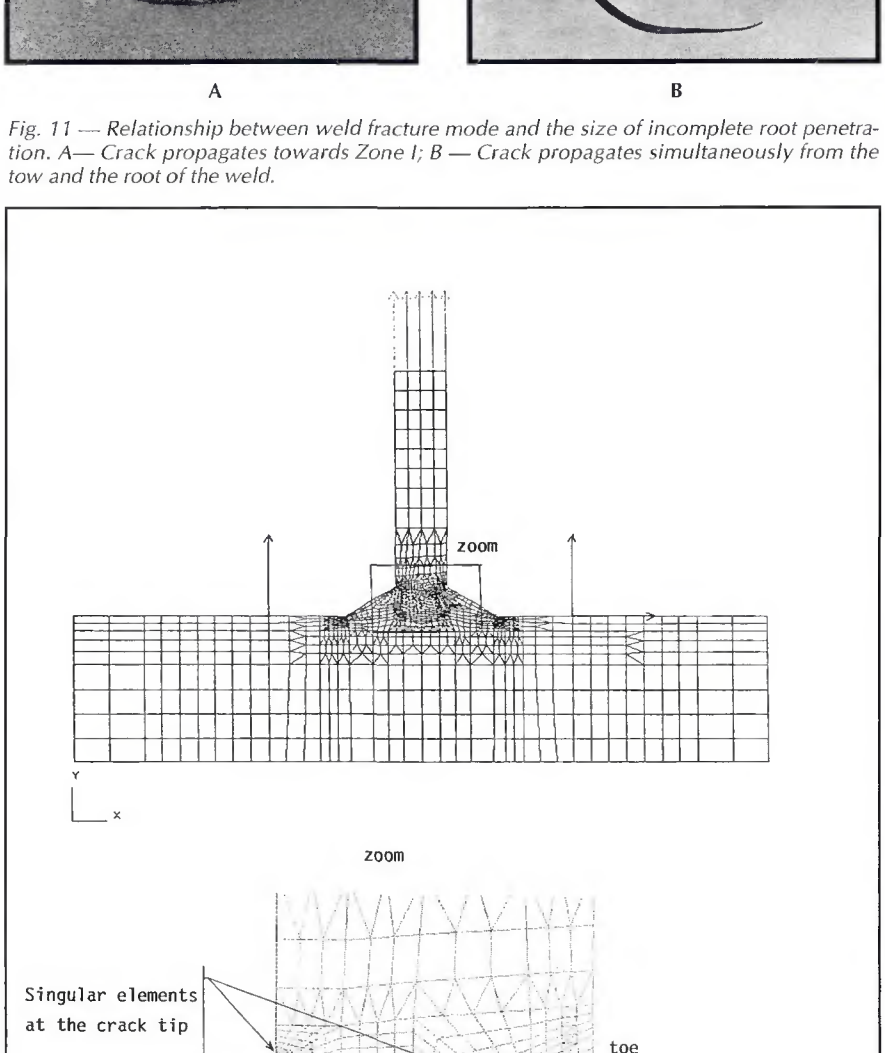

Fig. 12 — Two-dimensional calculations of boundary conditions. Singular elements at the crack tip used for determining stress intensity factors.

The theoretical propagation angle α (Fig. 13) was defined in the direction where the strain energy density was minimum (S min) with a positive local stress σαα.

This prediction method made it possible, for each propagation increment a + Δa, to determine a "fictive" crack propagating in the "pure" mode I.

The experimental program conducted for evaluating the fatigue behavior of Zone I of the weld has shown that only one fatigue-failure mode existed, whatever the extent of the incomplete penetration. The algorithm used for modeling the crack propagation path and for determining the stress intensity factor in mode I in this weld-zone is shown in Fig. 14.

The experimental work carried out for evaluating the fatigue behavior of the Zone II of the weld evidenced several fracture modes, which were dependent on the size of the incomplete penetration at the weld root. In that case, two different algorithms had to be considered.

1) The modeling of the crack path with 2a/t < 0.4 was carried out by applying the previous algorithm as presented in Fig. 14 (fatigue failure mode being the only possible mode in this case).

2) For simulating the crack path when 2a/t was between 0.4 and 0.9, it was necessary to modify the above-mentioned algorithm and to take into account the interaction effect between Zone II and Zone III of the weld. Consequently, the modeling must be achieved in this case by taking into consideration the simultaneous propagation of the cracks located in Zone II of the weld toe and on either side of the weld root.

In the hypotheses for the calculation, it was assumed that the cracks running in Zones II and III of the weld followed the same cracking law (like the Paris law $da/dN = C\,(\Delta K)^m$).

For this modeling, it was necessary to define arbitrarily an active crack and two passive cracks. The active crack was chosen in Zone II of the weld. This crack was increased with a constant increment, ai + 1 = ai + Δa. By integrating the PARIS law from the initial flaw ao through to the flaw ai + 1, the following was obtained:

$$N_p = \int_{a0}^{ai+1} C^{-1}(\Delta K)^{-m}\, da \qquad (4)$$

that is, the necessary number of cycles (N) for the crack to extend by the amount of (ai + 1 - ao).

Since the same law of cracking was applicable to cracks located at the weld root, we could determine the value of the propagation increment Δa (III) of each root crack, so that these cracks propagated within an identical number of cycles N.

Then the angle of fatigue crack deviation was defined in accordance with Sih's energy criterion. The relevant algorithm is shown in Fig. 15.

Numerical Application

This phase of numerical calculations demonstrated the effectiveness of the method when used for determining the fatigue crack propagation path at the toe and the root of the weld.

Although the calculation hypotheses were restrictive (calculations on the basis of linear elastic fracture mechanics assuming a homogeneous material without weld residual stresses), a fair approximation of the experimental crack

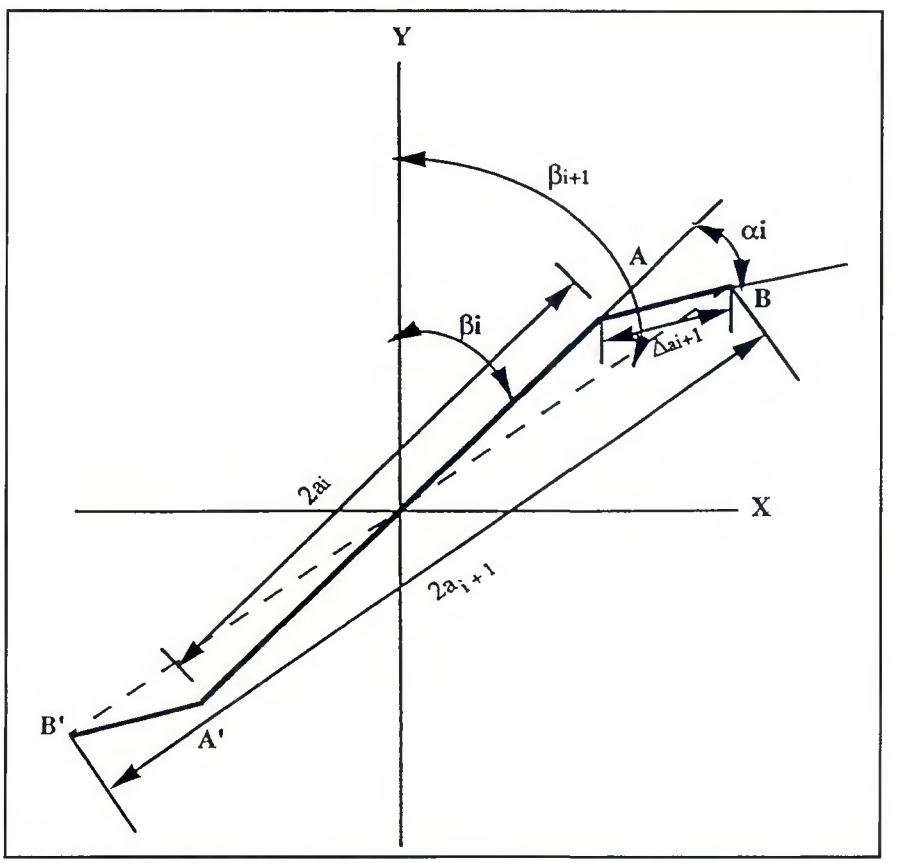

Fig. 13 — Theoretical propagation of angle α.

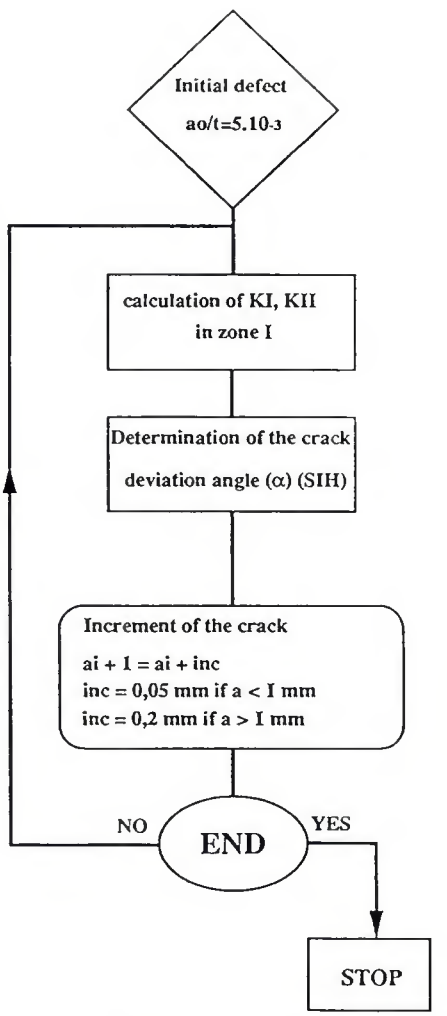

Fig. 14 — Algorithm used for modeling crack propagation path.

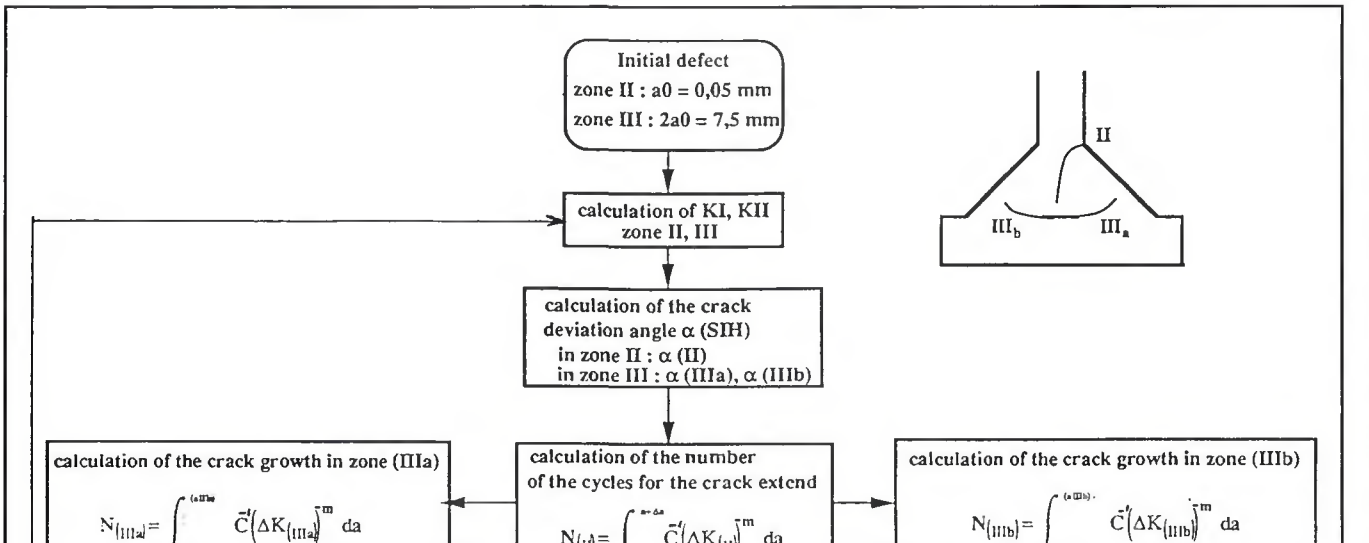

Fig. 15 — Algorithm used to determine the angle of fatigue crack deviation.

paths was obtained. For the failure modes considered (Zones I and II of the weld), see Figs. 16–18.

The modeling of the crack path in Zone II at the weld toe evidenced a correct reaction of the Sih's energy criterion for crack propagation (α) as a function of the size of the incomplete fusion at the root. Figure 19 illustrates the evolution KI = f(a/t) of each of the cracks in Zones II and III of the weld. The numerical values showed four succesive phases: 1)initially, an identical evolution of the cracks at the weld root was observed, 2) then an unbalance gradually appeared and reached a maximum when the crack located in the nearby Zone II approached the depth a/t = 0.3–0.4 in the weld, 3) from then on, a rebalancing of the evolution mode of the root cracks was observed when the crack in Zone II reached the mid-thickness of the welded plate, and 4) beyond that depth, the unbalance occurred in the reverse manner until the assembly failed.

Thus, the analysis of this numerical simulation demonstrated the existence of a constant interaction between these fatigue cracks at the onset of initiation, continuing throughout the propagation phase until complete failure of the weld occurred.

So interest in this kind of simulation was not only to permit the numerical determination of the (most likely) K functions of the cracks running in a welded assembly (or structure), but also to analyze (nearly cycle-by-cycle) the different phases of interaction between the cracks, as the fatigue failure proceeded.

Estimation of the Fatigue Life

Presentation and Formulation of the Analytical Model

The modeling of the fatigue behavior of fillet welded assemblies was based on the hypothesis that the cracks would follow a propagation law of the Paris type

$$\frac{da}{dN} = C\ (\Delta K)^m \qquad (5)$$

C and m materials constant

The stress intensity factor K (in mode 1) was determined by considering the real evolution of the shape of the crack front (for the assemblies welded by the SMAW and GMAW processes). In this case, the stress intensity factor K was expressed as K = K numerical x φ (a/c, a/t), φ (a/c ; a/t) being dependent on the form of the crack front.

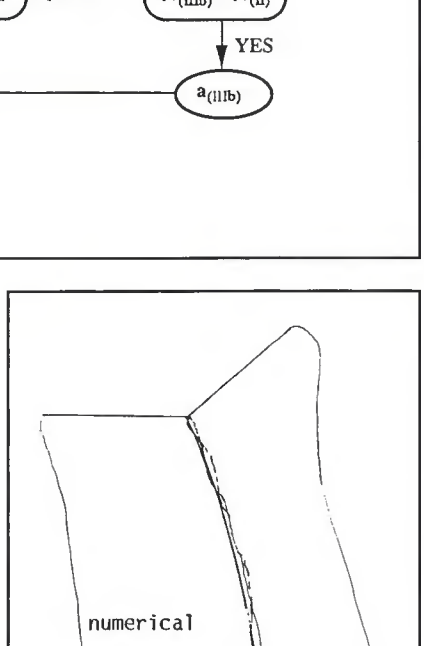

Fig. 16 — Modeling of the crack path in Zone I.

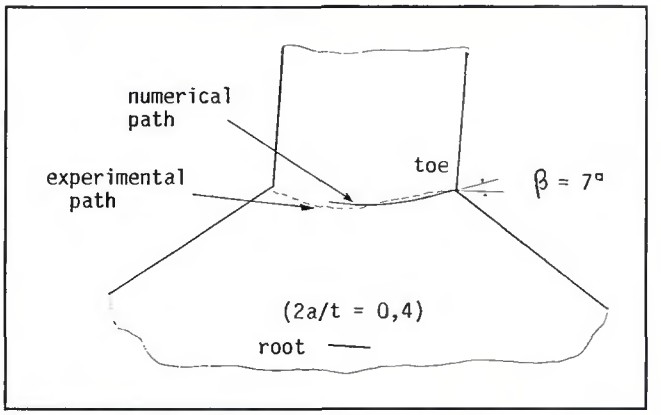

Fig. 17 — Modeling of the crack path in Zone II.

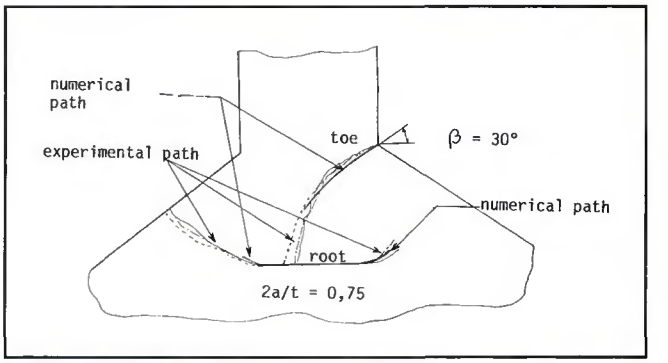

Fig. 18 — Simulation of the fatigue failure of the weld when a multiple failure mode is present.

The correction factor φ (Fig. 20) was defined by

$$\varphi(a/c,\ a/t)=\frac{KRN\ \text{plate}}{\text{K num. plate}} \quad \text{Fig. 20} \tag{6}$$

where KRN plate corresponds to the function K calculated with the model proposed by Raju-Newman (Ref. 5) for a flat plate subjected to tension or bending, and K num. plate corresponds to the function K obtained numerically with a flat plate subjected to tension or bending, with special consideration of the presence of a edge crack (a/c — > 0) in Zones I or II of the weld.

The Elber ratio that represents the relative fraction of the amplitude of the nominal load during which the crack is open is the following

$$U=\frac{\sigma_{max}-\sigma_{op}}{\sigma_{max}-\sigma_{min}} \tag{7}$$

The value of σ_{op} was derived from the method used for the monitoring of microcracks by microstrain gauges. Figure 4 shows clearly that the relation U = f(a/t) was relatively constant and high during the whole cracking stage.

Thus, the final expression for the stress intensity factor of the fillet welded assemblies was

$$\Delta K_{eff.\,joint}=U\times\Delta K_{num.\,joint}\times\frac{K_{RN\ plate}}{K_{num.\ plate}} \tag{8}$$

The number of cycles to failure was determined by integrating that relation

$$NR=\int_{ai}^{af}C^{-1}\left(U\times\Delta K_{num.\,joint}\times\frac{K_{RN\ plate}}{K_{num.\ plate}}\right)^{-m}da \tag{9}$$

Numerical Results

The calculations made in Zone I of the weld toe permitted the functions KI = f(a/t) to be defined for three distinct weld geometries. They were made by varying the toe angle only 30, 45, and 60 deg. For defining a unit evolution of the relation KI = f(a/t), the stress intensity factors were divided by the nominal stress applied in the weld. The following relation was obtained

$$\frac{K_{I\,num.\,joint}}{\sigma N_{fl}}=f(a/t) \tag{10}$$

The reference nominal stress (σN_{fl}) was calculated by the application of the strength of materials concepts for a beam subjected to three-point bending,

$$\sigma N_{fl}=\frac{mf}{l/v} \tag{11}$$

In the case of fillet welded assemblies, this nominal bending (flexural) stress (σN_{fl}) is induced by the loading span D. The numerical results corresponding to each case are presented in Fig. 21.

The numerical calculations made for studying Zone II of the weld permitted the determination of the functions KI = f(a/t) for two distinct sizes of incomplete fusion (2a/t = 0.4 and 0.75) by first ne-

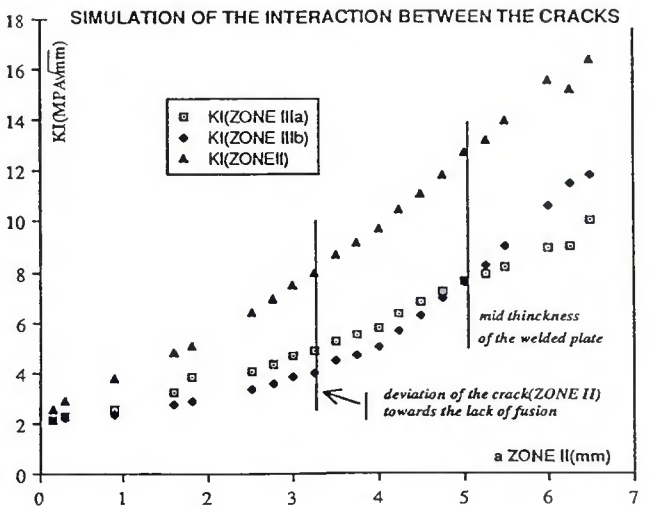

Fig. 19 — Evolution of cracks in Zones II and III.

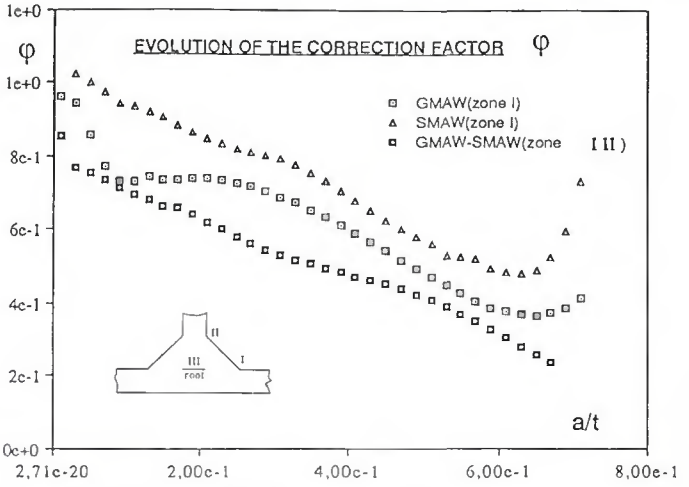

Fig. 20 — Evolution of the correction factor.

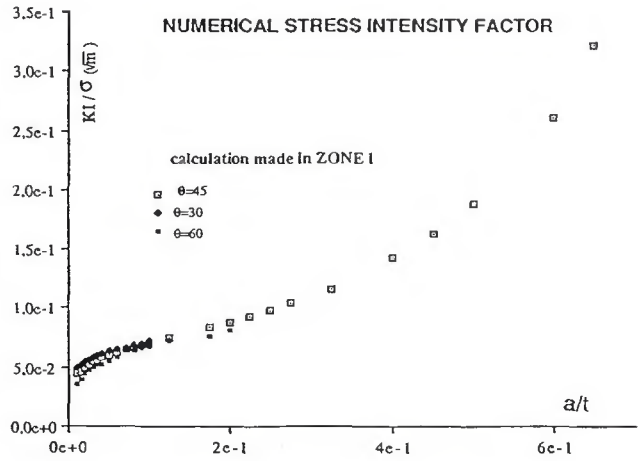

Fig. 21 — Numerical stress intensity factor for each case.

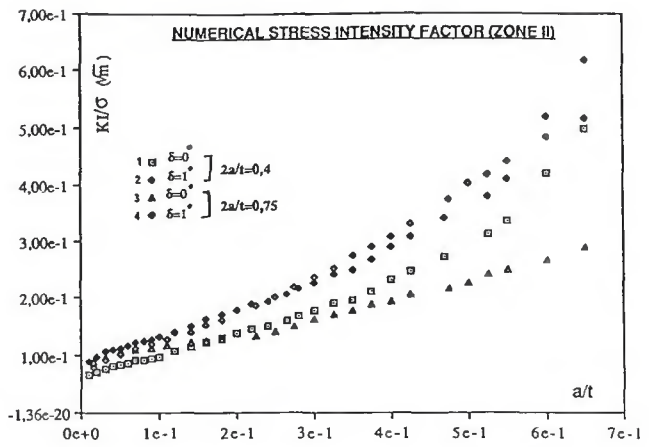

Fig. 22 — Stress intensity factor for Zone III.

glecting the residual deflection of the welded plates (δ = 0 deg), and then imposing a residual deflection of δ = 1deg (this value of δ = 1 deg corresponds to the maximum residual deflection measured experimentally on the test specimens).

The numerical values obtained for each case under study are presented in Fig. 22. The evolution of the stress intensity factor is also expressed by the relation

$$\frac{K_I\ joint,\ num}{\sigma_{NT}} = f(a/t) \qquad (12)$$

The reference nominal stress σ_{NT} in Zone II of the weld was determined by applying the strength of materials concepts to a flat plate subjected to uniaxial tension

$$\sigma_{NT} = \frac{F}{S} \qquad (13)$$

The analysis of the numerical results demonstrated the effect of the size of incomplete penetration on the value of the stress intensity factor KI during the whole cracking stage. In this case, an increase in the stresses in the weld zone of interest was observed when the size of the incomplete fusion increased (Fig. 22, curves 1, 3).

The analysis also demonstrated the effect of residual deflection (δ) between welded plates. In this case, the residual deflection induced a spurious bending stress, which was superimposed upon the tensile nominal stress applied to the fillet weld (Fig. 22, curves 1, 2).

The variation in the applied nominal stress in the fillet welds may then be expressed by relation in Equation 14 for welded joints containing an incomplete fusion of 2 a/t = 0.4 and 0.75. The evolution of this relation evidenced an initial increase in the values of KI to between 32 and 36%(depending on the fracture mode), which then fell to 14–23% when the crack reached a depth of a/t = 0.6.

$$\frac{K_I joint\ (\delta = 0°)}{K_I joint\ (\delta = 1°)} = f(a/t)\ \ (1) \qquad (14)$$

Thus, the deflection plays a dominant role in the scatter of the fatigue-life experimental data obtained from fillet welds subjected to tension and bending when the propagation of cracks extended from this zone of the weld.

Analytical Results

The modeling of the fatigue life of fillet welded assemblies subjected to tension and bending was made with special consideration of a function KI = f(a/t), depending on both the variation of the shape of the crack front and the fraction of crack opening during the whole propagation stage. The analytical functions K = f(a/c, a/t, U, θ) determined for the Zones I and II of the weld are presented in Fig. 23 for assemblies produced by the GMAW and SMAW processes.

The fatigue life was calculated by integrating the function KI = f(a/t) with special consideration of the fact that the cracks propagate according to a law of the Paris type. The integration bounds were defined by the limit of experimental detection (ao = 0.05 mm) and af was calculated by application of the linear elastic fracture mechanics concepts with special consideration of the limit value of the plastic yield of the remaining ligament. The materials constant C and m were determined experimentally with the E-36-4 base metal, transverse to the rolling direction ($C = 2–3.10^{-12}$, m = 3; for ΔK (MPa, √m)).

Analysis of the Analytical Results

The analytical values revealed a phase of slow crack extension (a < 1 mm) which, depending on the fracture zone (Zones I or II), represented 33 to 44% of the propagation life of the fillet welded assemblies — Table 3.

The modeling of the fatigue behavior of weld Zone 1 revealed an increase of nearly 80% in the propagation life when the toe angle θ was varied from 30 to 60 deg (the notch acuity decreased locally) — Fig 24.

The analytical study conducted in Zone II of the weld showed a decrease of nearly 50% in the propagation life of the assembly when the size of the incomplete penetration 2 a/t was varied from 0.4 to 0.75, and when we assumed a residual deflection between welded plates equal to δ = 0 deg and then δ = 1 deg — Fig. 25.

The results of evaluations of fatigue life made with this analytical model showed that in so far as the history of the fatigue behavior of the fillet welded assemblies was known (δapp., true δ, Na, Np = Nr-Na, fracture in Zones I or II, 2a/t), the calculated values approached the experimental results with a 28% mean error of estimate — Fig. 26.

Conclusions

The evaluation of the fatigue behavior of fillet welded assemblies subjected to tension-bending as a function of the weld penetration showed the following:

1) The method of detection by using micro-extensometers attached to the weld toe permitted the monitoring of small fatigue cracks, from the initiation stage (ai = 0.05 mm) through to a depth of 1 mm in the weld. The test results showed that this propagation phase of microdefects may represent from 30 to 90% of the fatigue life of the fillet welded

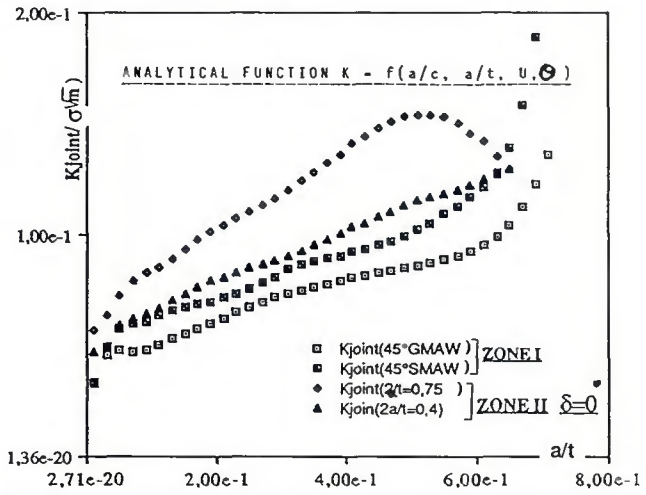

Fig. 23 — Analytic functions determined for Zones I and II.

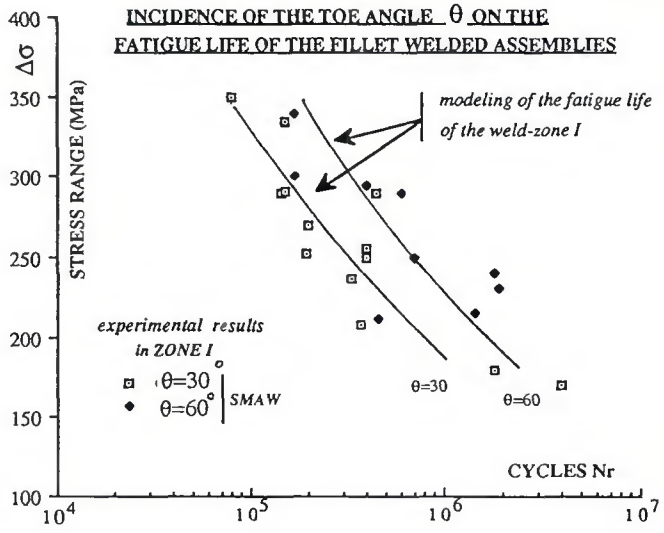

Fig. 24 — Increase in propagation life when toe angle varied from 30 to 60 deg.

assemblies, depending on the geometrical parameters, on the applied stress state and on the welding process used (GMAW or SMAW).

2) The synthesis of the test results revealed the existence of a critical size of incomplete penetration below which the incomplete penetration no longer exerted any significant effect on the fatigue life of fillet welded assemblies subjected to tension and bending. For assemblies produced with the GMAW and SMAW processes, this critical value was estimated at 2a/t = 0.8 (t = thickness of the welded plates) (Ref. 2).

Table 3 — Analytic Values for Crack Extension

	Rep	Δσ (MPa)	θ (deg)	N1 exp	Np exp	N1 cal	Np cal	N1/Np exp	N1/Np cal	Npexp-Npcal / Np exp (%)
	D6	283	44	2.1 E5	6.5 E5	2 E5	5.7 E5	0.32	0.36	−12
	A6	245	45	4 E5	1.2 E5	3.09 E5	8.9 E5	0.33	0.35	−25
GMAW	F5	270	30	1.6 E5	6.4 E5	1.94 E5	6 E5	0.25	0.32	+6
	F4	298	30	1 E5	2.8 E5	1.44 E5	4.47 E5	0.35	0.33	−59
	C5	243	53	4.4 E5	1.08 E6	4.75 E5	1.33 E6	0.40	0.35	−23
SMAW	MF2	230	49	2.69 E5	1.26 E6	2.7 E5	7.3 E5	0.22	0.37	+42
	MF3	231	59	2.83 E5	9.63 E5	1.47 E5	4.1 E5	0.30	0.36	+57
	MG1d	275	40	8.5 E5	2.18 E5	7.9 E5	2.16 E5	0.38	0.37	0.9
	MG1c	345	30	1.45 E5	3.7 E5	1.28 E5	3.77 E5	0.39	0.34	−1.8
GMAW and SMAW	I1	140	60	2.1 E5	3.8 E5	1.84 E5	4.5 E5	0.55	0.40	−18
	δ = 1°		2a/t = 0.7							
	I2	120	60	2.35 E5	4.3 E5	2.92 E5	7 E5	0.54	0.41	+62
	δ = 1°		2a/t = 0.7							
	I4	160	60	1.15 E5	4.1 E5	2.6 E5	5.8 E5	0.29	0.44	−41
	δ = 0°		2a/t = 0.7							

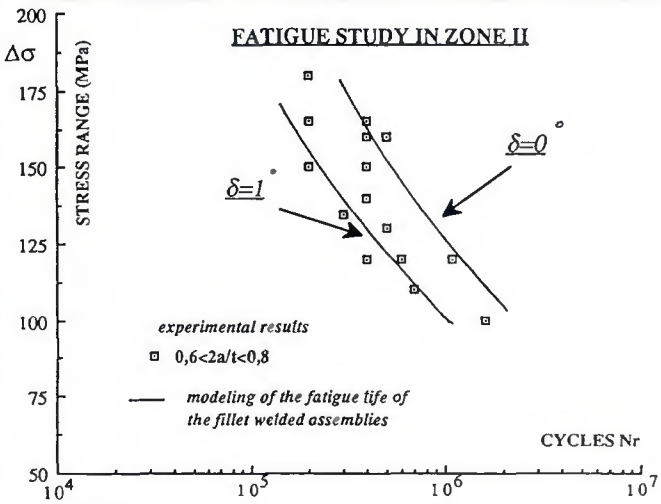

Fig. 25 — Fatigue study in Zone II revealed a decrease in propagation life.

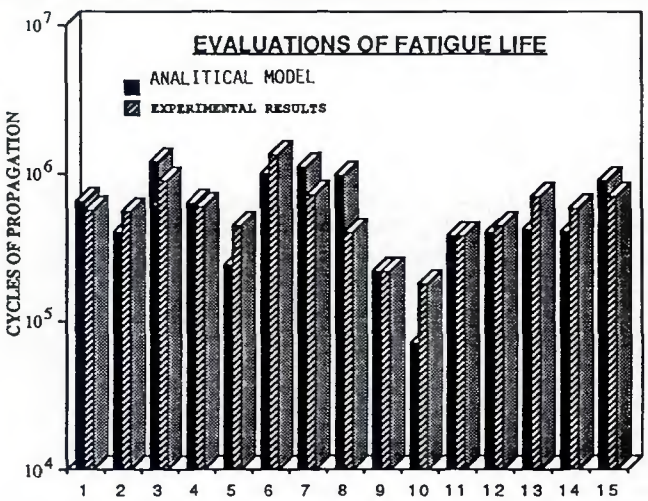

Fig. 26 — Comparison of calculated values with experimental results of fatigue life.

3) All the tests performed on load carrying fillet welded assemblies showed that the most restrictive stress condition for admitting a critical size for incomplete root-penetration corresponded to a uniaxial tension loading (Ref. 1).

In this case, the critical size of incomplete penetration below which the incomplete penetration no longer affected the fatigue behavior was 2a/t = 0.5 (t = thickness of welded plates).

4) Although the fatigue modeling of fillet welds is in itself a very complex physical problem (because of the presence of micro- and macro-heterogeneities of mechanical and structural nature, or of the presence of a very complex residual stress state), this study proved that the numerical calculations made by using the linear theory of elasticity (and the LEFM) permitted the following to be achieved: A) an evaluation of the preferred initiation-sites for fatigue microcracks in each sensitive zone of the weld as a function of the geometrical parameters and loading conditions, B) a simulation of the fatigue crack propagation paths, in each weld zone under study, by using the energy model proposed by Sih (Ref. 4), for a single or multiple failure mode of the fillet welded assemblies, and C) the modeling of the propagation life of fillet welded assemblies subjected to tension and bending, as a function of the geometrical parameters of the weld, of the size of incomplete penetration, of the residual deflection of the welded plates and of the welding process used (GMAW or SMAW).

5) The analysis of the results demonstrated the effectiveness of this analytical modeling which permitted the slow microcrack-propagation phase (evidenced by the experimental program) to be taken into account, and gave a satisfactory estimate of the fatigue life whatever the zone of failure and the welding process used.

References

1. Sahli, B., Leduff, I. A. 1986. Evaluation de la tenue en fatigue des joints soudes en croix en fonction de la penetration des soudures. Rapport IS No. 19637; contrat CETIM No. 852127.

2. Janosch, J. J. 1991. Etude de la tenue a la fatigue des assemblages en angle (en acier E36-4), en fonction de la dimension de la penetration des soudures, dans le cas d'une sollicitation combinee de traction et flexion. These de l'universite de Metz.

3. Elber, W. 1970. The significance of fatigue crack closure. ASTM STP 486, p. 230.

4. Sih, G. C. 1980. Mixed mode fatigue cracks growth prediction. *Engineering Fracture Mechanics,* Vol 13, pp. 439–451.

5. Newman, J. C., and Raju, I. S. 1981. An empirical stress intensity factor equation for the surface crack. *Engineering Fracture Mechanics,* Vol. 15, NASA, Hampton, U.S.A.

Appendix

θ	toe angle (deg)
H/t	throat thickness
T/t	thickness ratio of the weld plates
t	thickness of the weld plate (mm)
2a	incomplete penetration (mm), Zone III
ρ	weld toe radius (m)
δ	residual deflection of the welded plates (deg)
a	crack depth for a semi-elliptical surface crack (mm)
a0	initial crack defined by the limit of experimental detection (a0 = 5E-5m)
af	final crack (m) defined by LEFM
c	half crack length for a semi-elliptical surface crack (mm)
U	relative fraction of crack opening as define by Elber (Ref. 3)
σNT	nominal tensile stress (MPa)
σN_{fl}	nominal bending stress (MPa)
1σ	local main stress 1
σ_{op}	nominal stress during which the crack is open (MPa)
S	strain energy density
ν	Poisson's ratio
E	Young's modulus (MPa)
μ	shear modulus (MPa)
α	theoretical propagation angle (deg) defined by Sih (Ref. 4)
C, m	materials constant
β	propagation angle of the cracks at the weld toe (deg)
φ	correction factor, dependent on the form of the crack front
KRN plate	K calculated with the model proposed by Raju/Newman (Ref. 5) (MPa $\sqrt{m}$)
Knum.	joint stress intensity factor obtained numerically for an edge crack of the fillet weld assemblies (Zones I, II, III) (MPa x $\sqrt{m}$)
Knum. plate	stress intensity factor obtained numerically for an edge crack in a flat plate (MPA $\sqrt{m}$)